Supporting Information for:

Atomic Substitution Enabled Synthesis of Vacancy-Rich Two-Dimensional Black TiO_{2-x} Nanoflakes for High-Performance Rechargeable Magnesium Batteries

Authors:

Yanrong Wang,[†] Xiaolan Xue,[†] Pingying Liu,[‡] Caixing Wang,[†] Xu Yi,[†] Yi Hu,[†] Lianbo Ma,[†] Guoyin Zhu,[†] Renpeng Chen,[†] Tao Chen,[†] Jing Ma,[†]* Jie Liu[†,§] and Zhong Jin[†]*

Affiliations:

[†] Key Laboratory of Mesoscopic Chemistry of MOE, School of Chemistry and Chemical Engineering, Nanjing University, Nanjing, Jiangsu 210023, China.

[‡] School of Materials Science and Engineering, Jingdezhen Ceramic Institute, Jingdezhen 333403, China.

[§] Department of Chemistry, Duke University, Durham, NC 27708, USA.

*Address correspondence to: majing@nju.edu.cn (Prof. J. Ma); zhongjin@nju.edu.cn (Prof. Z. Jin)

Supporting Figures

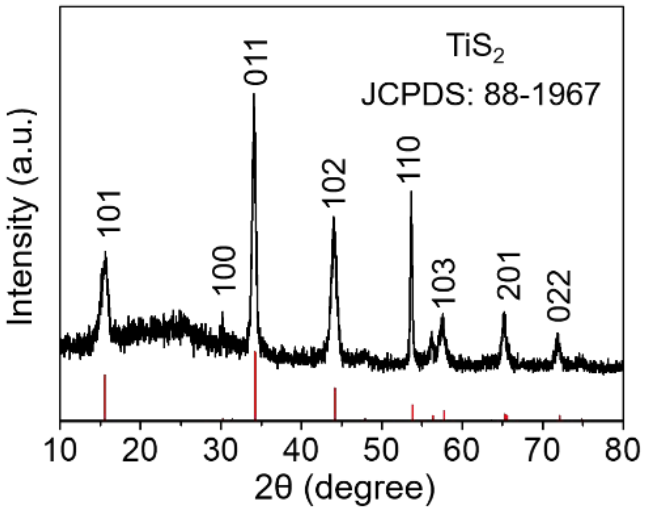

Figure S1. XRD pattern of ultrathin TiS_2 nanoflakes.

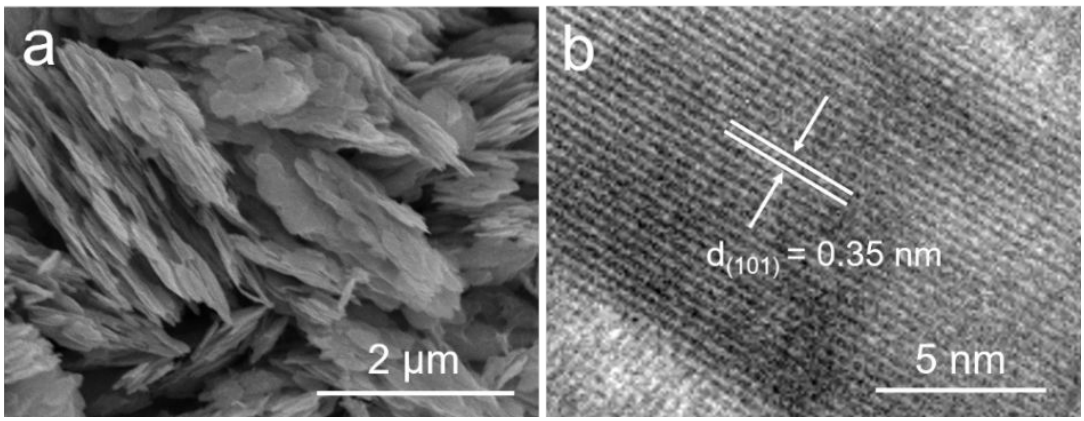

Figure S2. (a) SEM image and (b) HRTEM image of W-TiO_2 nanoflakes as a control sample.

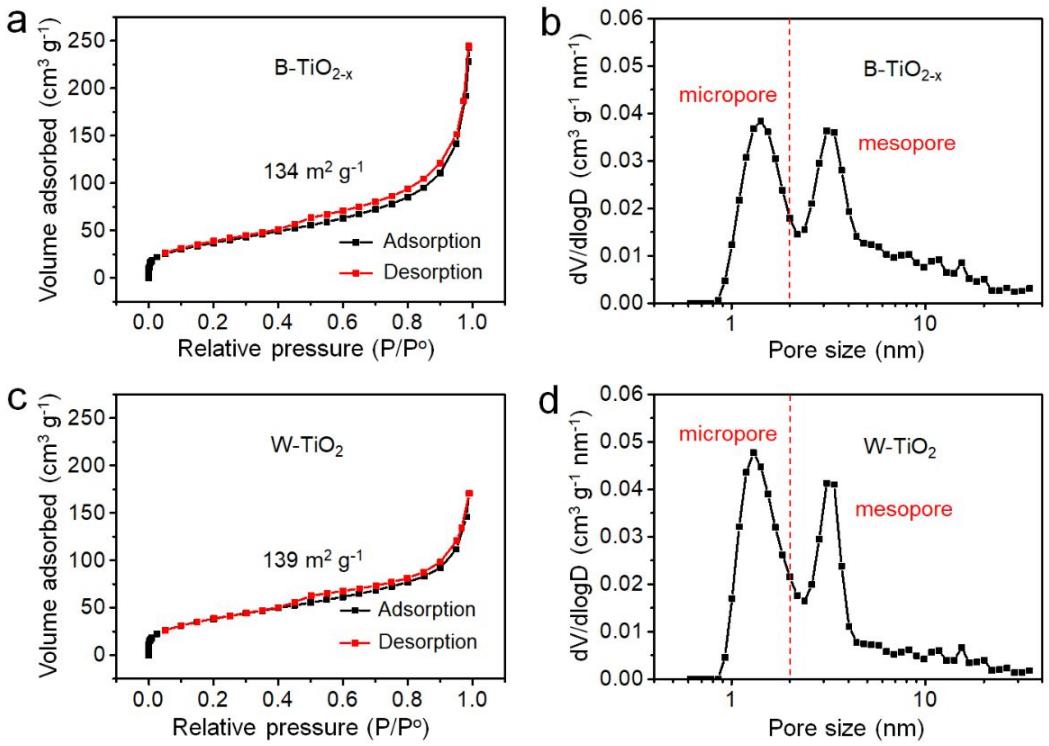

Figure S3. Nitrogen sorption-desorption isotherms and pore-size distributions of (a, b) porous B-TiO_{2-x} nanoflakes and (c, d) W-TiO_2 control sample, respectively.

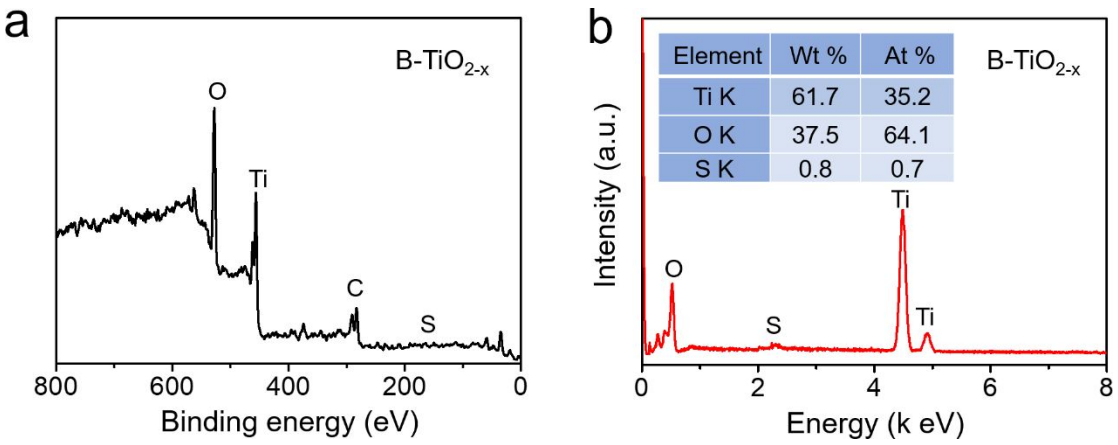

Figure S4. (a) Survey XPS spectrum, (b) EDX analysis of B-TiO_{2-x} nanoflakes.

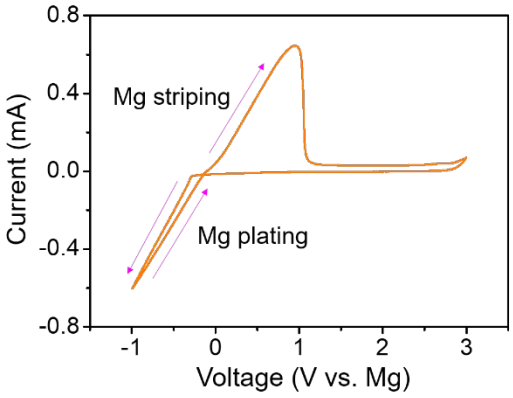

Figure S5. Cyclic voltammograms (CV) profile of Mg stripping/plating measured at a scan rate of 25 mV s^{-1} with a three-electrode testing system based on the counter and reference electrodes of magnesium foils, the working electrode of platinum plate, and 0.4 M APC/THF electrolyte.

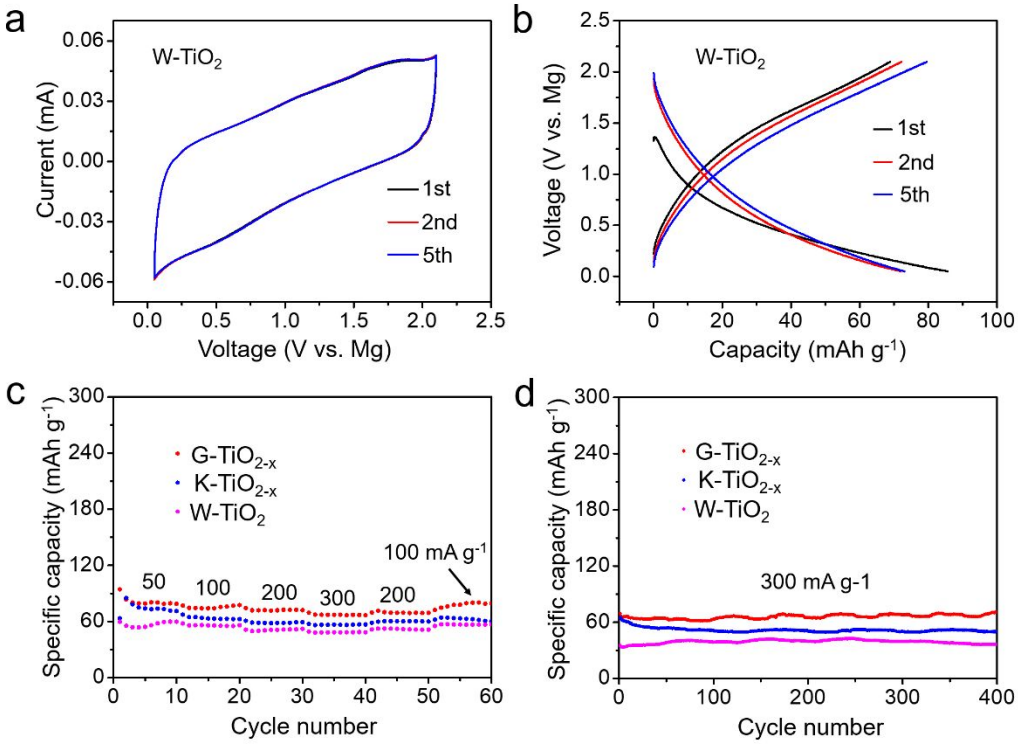

Figure S6. (a) CV curves of W-TiO_2 control sample at a scan rate of 0.2 mV s^{-1}. (b) Discharge-charge voltage profiles of W-TiO_2 control sample at a current density of 50 mA g^{-1}. (c) Rate performance of the control samples with different OV content prepared by annealing in air for different periods (1 h, 2 h, 4 h). (d) Cycling performance of these control samples at 300 mA g^{-1}.

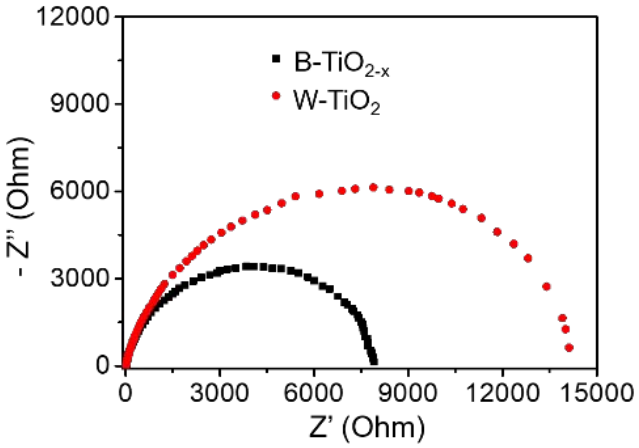

Figure S7. EIS curves of porous B-TiO_{2-x} nanoflakes and W-TiO_2 control sample.

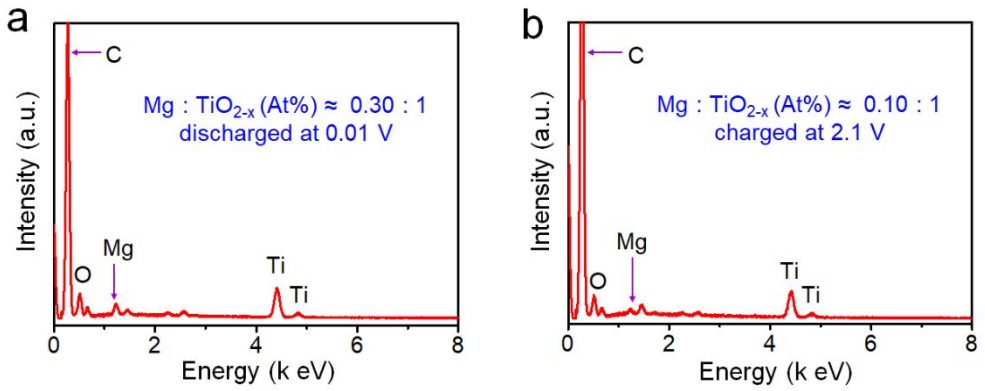

Figure S8. EDX spectra of porous B-TiO_{2-x} nanoflakes anode (a) after the 1st discharge step and (b) after the 1st charge step.

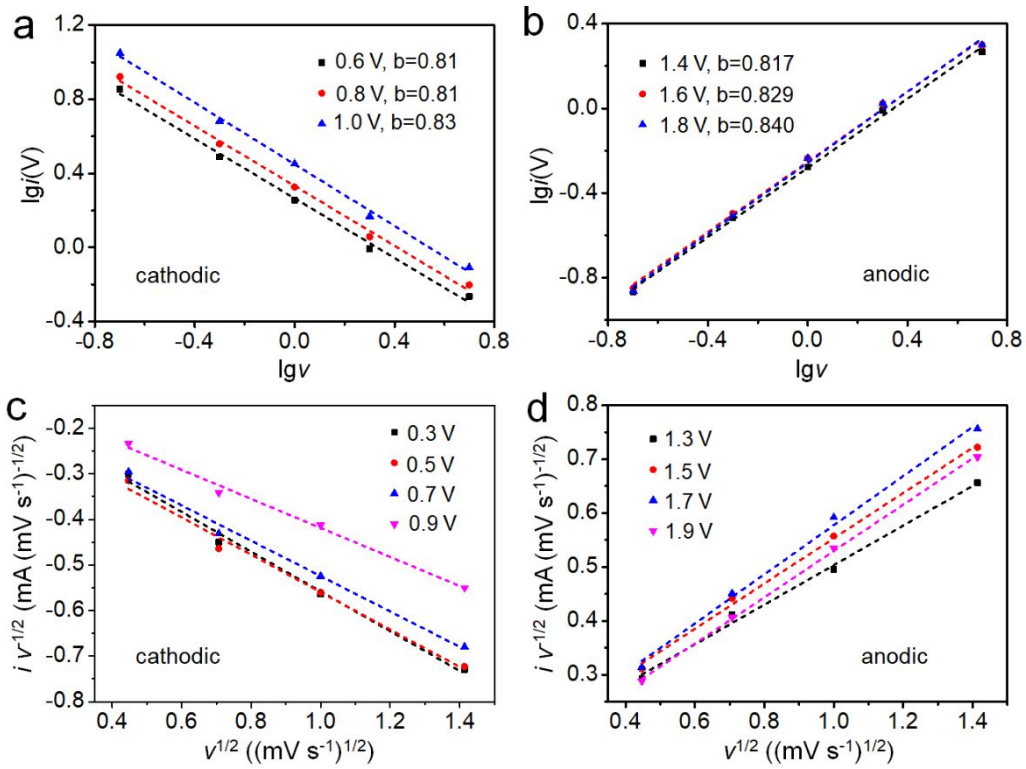

Figure S9. (a,b) Plots of lg*i* *vs.* lg*v* at various sweep rates based on lg*i*(V) = *b*lg*v* + lg*a*. (c,d) Plots of $iv^{-1/2}$ *vs.* $v^{1/2}$ at specific voltages during the discharge and charge processes with the values of *v* varies from 0.2 to 2.0 mV s^{-1}.

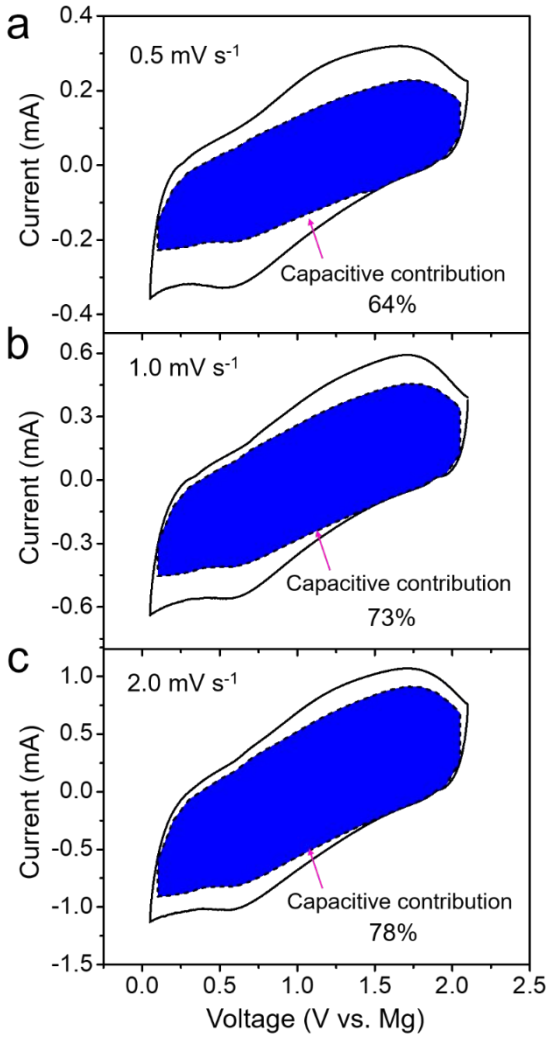

Figure S10. Capacitive contributions (corresponding to the shaded areas) on the total capacities at the scan rates of (a) 0.5, (b) 1.0, and (c) 2.0 mV s^{-1}, respectively, calculated based on the equation: $i(V) = k_1v + k_2v^{1/2}$.

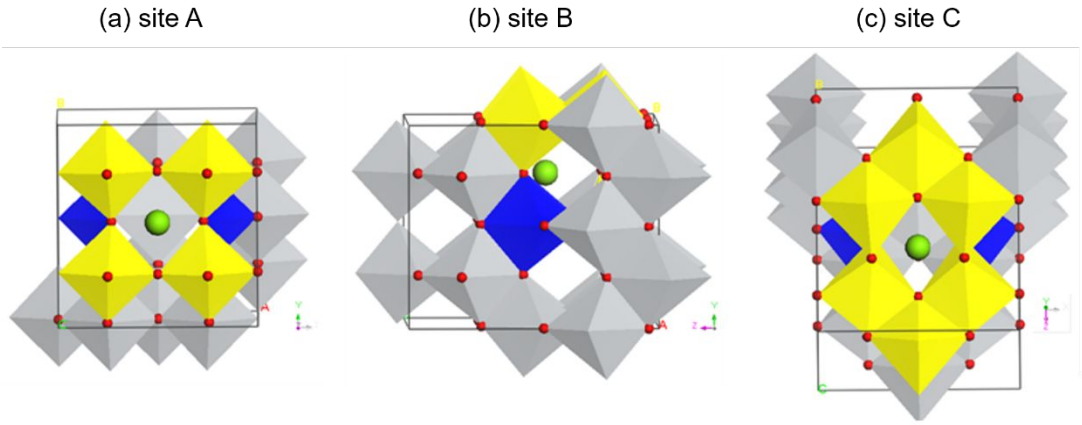

Figure S11. Three different insertion sites for one Mg^{2+} ion in the structure of B-TiO_{2-x}: (a) site A, (b) site B, and (c) site C. The gray and yellow octahedra represent the Ti^{4+}-O octahedra, and the blue octahedra represents the Ti^{3+}-O octahedra, respectively. The green and red balls represent the Mg and O atoms.

Supporting Tables

Table S1. Comparison of Mg^{2+} storage performances of vacancy-rich B-TiO_{2-x} nanoflakes in this work with other previously-reported anode materials for Mg batteries.

Ref.	Anode material	Electrolyte	Potential range (*vs.* Mg^{2+}/Mg)	Initial discharge capacity	Discharge voltage (*vs.* Mg^{2+}/Mg)	Long-term cycling stability
This work	**vacancy-rich B-TiO_{2-x} nanoflakes**	**0.4 M APC in THF**	**0.05−2.1 V**	**190 mA h g^{-1} at 50 mA g^{-1}**	**Average discharge voltage ~0.5 V**	**77 mA h g^{-1} at 300 mA g^{-1} after 400 cycles**
(22)	$Li_4Ti_5O_{12}$	0.25 M $Mg(AlCl_2EtBu)_2$ in THF	0−1.85 V	155 mAh g^{-1} at 15 mA g^{-1}	~0.5 V	55 mA h g^{-1} at 300 mA g^{-1} after 500 cycles
(47)	ultrathin TiO_2 nanowires	0.4 M APC in THF	0.01–2.0 V	142 mAh g^{-1} at 10 mA g^{-1}	---	37 mA h g^{-1} at 200 mA g^{-1} after 500 cycles
(49)	cation-deficient anatase TiO_2	0.2 M APC in THF	0.05–2.3 V	165 mA h g^{-1} at 20 mA g^{-1}	~0.5 V	65 mA h g^{-1} at 300 mA g^{-1} after 500 cycles
(50)	$Na_2Ti_3O_7$ nanoribbons	0.25 M APC in THF	0.01-2.0 V	135 mAh g^{-1} at 20 mA g^{-1}	---	53 mA h g^{-1} at 200 mA g^{-1} after 500 cycles
(18)	Sn	0.4 M APC in THF	0-0.8 V	275 mAh g^{-1} at 50 mA g^{-1}	discharge plateau ~0.14 V	---
(18)	SnSb	0.4 M APC in THF	0-0.8 V	420 mAh g^{-1} at 50 mA g^{-1}	discharge plateau ~0.17 V	~270 mA h g^{-1} at 500 mA g^{-1} after 200 cycles
(51)	Bi	$Mg(N(SO_2CF_3)_2)_2$ in ACN	0.02-0.6 V	330 mAh g^{-1} at 35 mA g^{-1}	discharge plateau ~0.25 V	220 mA h g^{-1} at 350 mA g^{-1} after 100 cycles
(52)	SnSb-graphene	APC	0-0.8 V	420 mAh g^{-1} at 50 mA g^{-1}	discharge plateau ~0.16 V	260 mA h g^{-1} at 500 mA g^{-1} after 200 cycles

Table S2. The atomic ratios of Ti^{4+} and Ti^{3+} species calculated by the Ti 2p peak areas in the XPS spectra of B-TiO_{2-x} nanoflakes anode at different discharge-charge states.

Discharge-charge states	Ti^{4+}	Ti^{3+}
Freshly-prepared (B-TiO_{2-x})	80%	20%
After the 1st discharge step (B-TiO_{2-x})	52%	48%
After the 1st charge step (B-TiO_{2-x})	67%	33%

Table S3. The calculated lattice constants, energies and the relative formation energies of different kinds of Mg_nTiO_{2-x}.

Formula	Concentration		Lattice Parameters						Energy per TiO_2	Relative Formation Energy $E_{formation}$
	OV	Mg^{2+}	*a*/Å	*b*/Å	*c*/Å	*α*/°	*β*/°	*γ*/°	(eV)	meV/ TiO_2
TiO_2 (exp.)	0	0	7.57	7.57	9.51	90	90	90		
TiO_2 (cal.)	0	0	7.60	7.60	9.71	90	90	90	-2481.573	
TiO_{2-x}	0.0312	0	7.61	7.61	9.71	90	90	90	-2454.104	
Mg^{2+} ions insertion										
$Mg_{0.06}TiO_{2-x}$_a	0.0625		7.66	7.77	9.58	90	90	90	**-2515.018**	0
$Mg_{0.06}TiO_{2-x}$_b	0.0625		7.67	7.75	9.56	90	90	90	-2515.016	0
$Mg_{0.06}TiO_{2-x}$_c	0.0625		7.76	7.64	9.67	90	90	90	-2514.984	0
$Mg_{0.12}TiO_{2-x}$_a	0.125		7.68	7.96	9.39	90	90	90	**-2575.946**	**-14.25**
$Mg_{0.12}TiO_{2-x}$_b	0.125		7.70	7.98	9.42	90	90	90	-2575.926	5.61
$Mg_{0.12}TiO_{2-x}$_c	0.125		7.87	7.87	9.38	90	90	90	-2575.912	19.51
$Mg_{0.18}TiO_{2-x}$_a	0.187		7.69	8.11	9.34	90	90	90	**-2636.862**	**-3.35**
$Mg_{0.18}TiO_{2-x}$_b	0.187		7.82	8.06	9.21	90	90	90	-2636.836	22.39
$Mg_{0.18}TiO_{2-x}$_c	0.187		7.87	7.94	9.36	90	90	90	-2636.796	62.60
$Mg_{0.24}TiO_{2-x}$_a	0.250		7.80	8.13	9.26	90	90	90	**-2697.777**	**-1.81**
$Mg_{0.24}TiO_{2-x}$_b	0.250		8.16	7.94	9.00	90	90	90	-2697.768	7.63
$Mg_{0.24}TiO_{2-x}$_c	0.250		8.02	8.03	9.04	90	90	90	-2697.754	21.32

Table S4. Calculated energy barriers and migration distances of one Mg^{2+} ion migration between three different sites in the supercell of B-$TiO_{2-x.}$

Migration path	Migration energy barrier (eV)	Migration distance (Å)
Path site B → site A	1.02	3.92
Path site C → site A	0.51	3.80
Path site C → site B	0.11	1.59